

Specific Binding of Integrin $\alpha_{IIB}\beta_3$ to RGD Peptide Immobilized on a Nitrilotriacetic Acid Chip: a Surface Plasmon Resonance Study

Y.-J. Lu, F. Zhang, and S.-F. Sui*

Department of Biological Sciences and Biotechnology, State Key Laboratory of Biomembranes, Tsinghua University,
Beijing 100084, P. R. China; fax: (86) 10-62784768; E-mail: suisf@mail.tsinghua.edu.cn

Received December 4, 2001

Revision received January 16, 2002

Abstract—Nitrilotriacetic acid has been routinely used in protein purification for its high affinity for His-tagged protein in the presence of Ni^{2+} . Here we reported a type of nitrilotriacetic acid chip (NTA-chip) prepared by transferring NTA-DOGS containing a lipid monolayer to a 50 nm thick gold layer deposited on a glass slide. The surface binding ability of His-tagged protein and regeneration of NTA chip were characterized using a synthetic polypeptide P1 (His-His-His-His-His-His- ϵ -amino-hexanoic-Gly-Gly-Arg-Gly-Asp-Ser). The effect of divalent cations on integrin binding affinity for RGD ligand was investigated after P1 had been immobilized onto the sensor chip. The results show that the NTA-chip is a useful tool to immobilize His-tagged protein on the chip surface, and can provide a functional orientation for further investigation. The results also show that removing of Ca^{2+} bound on low affinity sites or adding of Mn^{2+} can increase the binding ability of integrin.

Key words: nitrilotriacetic acid, surface plasmon resonance, RGD, integrin $\alpha_{IIB}\beta_3$, His-tagged peptide

Integrin $\alpha_{IIB}\beta_3$, a calcium-dependent heterodimeric protein on platelets, can mediate platelet aggregation by binding to its receptors. The receptors include fibrinogen [1], fibronectin [2], vitronectin [3], and von Willebrand factor [4] that contain RGD sequence that can be recognized by integrin $\alpha_{IIB}\beta_3$ [5]. There are several divalent cation binding motifs in integrin $\alpha_{IIB}\beta_3$, which can bind Ca^{2+} , Mg^{2+} , and Mn^{2+} specifically [6-15]. These divalent cations play an important role in regulating integrin function and ligand binding property. Among them, Ca^{2+} is the most important [7]. Integrin has two classes of Ca^{2+} binding sites, one site with high affinity (nM) and 3-4 sites with low affinity (μM) [8]. The binding of Ca^{2+} to the high affinity site is necessary for dimer formation [7], and such binding can promote the binding of integrin $\alpha_{IIB}\beta_3$ to its ligand [9]. However, high concentration of Ca^{2+} (5 mM) lead to a dissociation of bound RGD containing ligand

Fab-9 from integrin [9], which suggests an inhibitory effect on ligand binding of low affinity Ca^{2+} binding sites. Mn^{2+} was reported to be a potent regulator in several integrin-mediated cell adhesion events [10, 11]. It has been reported that Mn^{2+} can increase the binding activity of integrin to RGD peptide [12, 13] and cyclic-HarGD [6], while decreasing the binding activity of integrin to fibrinogen [12, 14]. Though the crystal structure of integrin α_M subunit has provided a certain insight in the Mn^{2+} binding site [15], further investigations are still needed for revealing its physiological role.

Surface Plasmon Resonance (SPR) has emerged as a useful tool for obtaining thermodynamic and kinetic information on biochemical reactions occurring at or near an interface for label-free and real time measurement [16]. It permits the measurement of the mass change of deposited material with a high degree of accuracy. To prepare a SPR biosensor chip the supported planar lipid film has been widely used [17, 18]. Based on the solid supported planar lipid film the SPR technique has been extensively used to characterize lipid layer properties [19, 20], protein-protein interactions [21, 22], DNA-protein interactions [23, 24], and membrane-protein interactions [25-27]. Both the binding constant and the stoichiometry of the interaction can be analyzed by SPR.

Abbreviations: DPPG) dipalmitoylphosphatidylglycerol; DOPC) dioleoylphosphatidylcholine; LB) Langmuir-Blodgett; SPR) Surface Plasmon Resonance; NTA) nitrilotriacetic acid; NTA-DOGS) N_α, N_α -bis(carboxymethyl)- N_ϵ -(1,2-dioleoyl-*sn*-glycero-3-succinyl)-L-lysine; RGD) Arg-Gly-Asp; RU) Response Unit; P1) His-His-His-His-His-His- ϵ -aminohexanoic-Gly-Gly-Arg-Gly-Asp-Ser.

* To whom correspondence should be addressed.

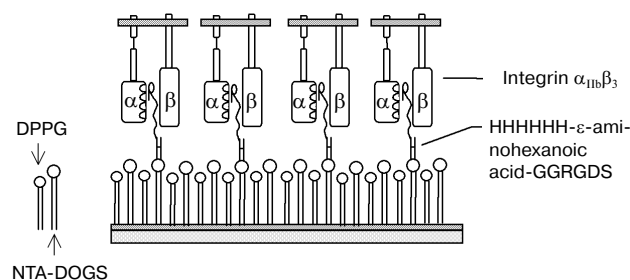


Fig. 1. Schematic model of our experiment. As indicated in the figure, after the mixed monolayer was transferred to the sensor chip, His-tagged peptide was added into the chamber to bind to NTA-DOGS. Then integrin will interact with the RGD head group in the C-terminal of the peptide.

Nitrilotriacetic acid (NTA), which was first introduced by Hochuli *et al.*, is widely used as a metal-affinity column material to purify His-tagged proteins [28]. NTA-lipids, were synthesized and characterized by two groups [29, 30], and the studies using GFP or fluorescence-labeled His-tagged protein demonstrated that His-tagged proteins could specifically bind to NTA-lipid domains [31, 32]. The reversible and functional immobilization of His-tagged protein on NTA-lipid surface has been used to control protein orientation and to form two-dimensional crystals of proteins [33–36]. The self-assembly of NTA-lipid and the immobilization of NTA to dextran matrix have been characterized [37, 38].

Here, we present a method for transferring NTA-DOGS containing lipid monolayer to solid support to prepare an NTA-chip for SPR. Using a synthetic peptide containing both His-tagged peptide and RGD group, HHHHHH- ϵ -aminohexanoic-GGRGDS (P1), we studied the specific interaction of integrin and RGD ligand and effect of Ca^{2+} and Mn^{2+} on integrin ligand binding affinity. The schematic model is shown in Fig. 1. Our results show that integrin binds to P1 in a specific manner, removing of Ca^{2+} from the low binding affinity site and adding Mn^{2+} will promote the binding of integrin to RGD ligand. The results also indicate that Mn^{2+} may bind to the low affinity Ca^{2+} binding site.

MATERIALS AND METHODS

Chemicals and peptides. NTA-DOGS was purchased from Avanti Polar Lipids (USA), DPPG and DOPC were purchased from Sigma (USA). The peptide P1 and GRGDSP were synthesized by Anaspec (USA), and the purities were determined to be over 95%. Other chemicals were purchased locally. Integrin $\alpha_{\text{IIb}}\beta_3$ was purified from human platelets according to the method of Fitzgerald *et al.* [39]. Purified integrin $\alpha_{\text{IIb}}\beta_3$ was dialyzed to buffer A (0.1% Triton X-100, 20 mM Tris-HCl, pH 7.4, 100 mM

NaCl, 1 mM Ca^{2+} , 1 mM Mg^{2+}), and then stored at -80°C . The purity of integrin was examined by sodium dodecyl sulfate polyacrylamide gel electrophoresis.

π -A isotherm of NTA-DOGS monolayer. Film balance measurement was performed on a computer controlled Langmuir–Blodgett (LB) trough. The LB trough has a volume of 168 ml, and a surface area of 202.5 cm². A moveable barrier was used to change the area that was covered by the lipid monolayer, and a Willhelmy system was used to measure the surface tension. Phospholipid dissolved in an organic solution (chloroform–methanol, 3 : 1 v/v) was carefully spread on the surface of buffer in the trough. After 30 min, the monolayer was compressed. Pressure/area diagrams of lipid monolayers were obtained by isothermal compression. All experiments were performed at room temperature ($25 \pm 1^\circ\text{C}$).

Preparation of NTA-containing supported monolayer. Supported membranes constitute a widely used model membrane system in studying lipid/protein interactions [40]. In the present work, supported monolayers on gold-coated cover slides were prepared according to the methods described by Sui *et al.* [18]. After a 50 nm thick gold film was deposited onto the slide under vacuum condition, a lipid monolayer at a surface pressure of 42 mN/m was horizontally transferred onto the slide by hand. Pure NTA-DOGS monolayer was used in the study of P1 interaction with the NTA-chip, while a mixture of NTA-DOGS/DPPG (1 : 1) was used when studying divalent cations effects on integrin ligand binding ability.

Surface Plasmon Resonance setup. A homemade SPR system [18, 41] based on the Kretschman configuration was used in present work. A HL6711G semiconductor laser (China; wavelength of 670 nm) was used as the incident polarized light source, and a photodiode served as a detector to collect the reflected light. The sensor chip was stuck onto a prism with refractive index of 1.8 through an index matching oil (cedar wood oil, $n = 1.515$). A 200- μl sample chamber was made of Teflon. The sample chamber was rotated by a computer-controlled stepping motor with a minimum step angle of $1/36,000^\circ$. Each curve of response-unit versus time was obtained by varying the incident angle around the resonance point with an error of less than 0.001° . All experiments were performed at room temperature ($25 \pm 1^\circ\text{C}$).

SPR experiments design. Buffer B (20 mM Tris-HCl, pH 7.4, 100 mM NaCl, 1 mM Ni^{2+} , 1 mM Ca^{2+} , 1 mM Mg^{2+}) was used in the experiments to investigate P1 interaction with NTA-chip. After the NTA-chip was balanced with buffer B, 20 μl 1% bovine serum albumin (BSA) was added into the chamber to block the nonspecific binding of P1 to the surface. Thirty minutes later, buffer B was used to wash out the excess BSA. Then P1 with concentrations from 0.17 to 5.4 μM was added into the chamber separately to carry out the binding analysis. The apparent dissociation constant of P1 was calculated by a double inverse linear rearrangement of the adsorption isotherm [42, 43].

The binding of integrin $\alpha_{IIb}\beta_3$ to P1 was carried out in buffer C (20 mM Tris-HCl, pH 7.4, 100 mM NaCl, 1 mM Mg^{2+}) with different composition of divalent cations. A series of buffers (buffer C; buffer C with 1 mM EGTA, 1 mM Mn^{2+} , 1 mM Ca^{2+} , or 1 mM Mn^{2+} /1 mM Ca^{2+}) were used in the experiments to get different binding performance of integrin in the presence of different divalent cations. After P1 was immobilized onto the sensor surface, the sensor chip was balanced with buffer. Then the binding of integrin was carried out with 0.02 mg/ml integrin in the running buffer containing 0.01% Triton X-100. To evaluate the role of Ca^{2+} binding site in integrin ligand binding, the integrin had been dialyzed against buffer D (0.1% Triton X-100, 20 mM Tris-HCl, pH 7.4, 100 mM NaCl, 1 mM Mg^{2+}) at 4°C overnight [7].

RESULTS

π -A isotherm of NTA-DOGS monolayer. To test the binding activity of NTA-lipid monolayer, a film balance measurement was performed. The π -A isotherm of NTA-DOGS in the presence or absence of 3 mM imidazole was measured as shown in Fig. 2. From Fig. 2 we can see that in the presence of 3 mM imidazole, the whole π -A curve shifts up with an increase in the axis of area. An average increased area of 16.7 \AA^2 per NTA-DOGS molecule in the surface tension range from 20 to 40 mN/m can be obtained. A control experiment showed that imidazole had no effect on the DOPC monolayer (result not shown).

Characterization of NTA-chip. After NTA-DOGS had been transferred onto the gold surface, the surface binding activity of His-tagged peptide was characterized. As reported by Hainfeld et al. [44], 10–40 mM imidazole was used to inhibit the unspecific adsorption of native histidine in proteins to NTA and 100 mM imidazole could inhibit the specific binding of His-tagged protein to NTA. Therefore, buffers containing 30- and 100-mM imidazole were used in the experiments to investigate the binding of P1 to NTA. From Fig. 3, we can see that in the presence of 30 mM imidazole, the binding amount of P1 decreases to 90 RU compared to 120 RU in the buffer without imidazole. While in the presence of 100 mM imidazole, nearly all the binding of P1 is eliminated from the interface, and only a very small amount (15 RU) of P1 is retained on the NTA-chip.

The NTA-chip can be regenerated by washing with EDTA and then incubating in Ni^{2+} buffer. After the binding of P1 to NTA-chip reached equilibrium, 10 mM EDTA was used to detach the bound P1 from the NTA-chip. Then the chip was regenerated by incubation in 1 mM Ni^{2+} buffer for 30 min. After that, P1 was added to execute the rebinding process. Three cycles of regeneration were carried out, as shown in Fig. 4. From the plot,

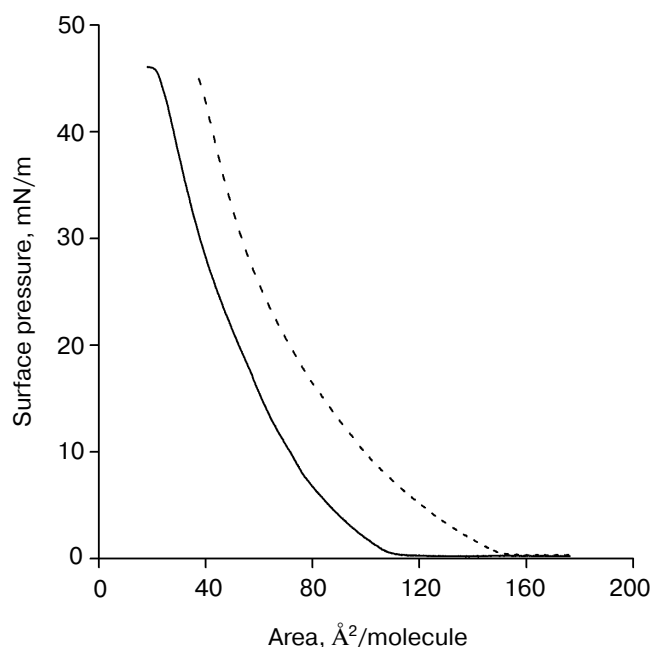


Fig. 2. Effects of imidazole on the isotherm of NTA-DOGS monolayer. Subphase: 20 mM Tris-HCl, pH 8.0, 100 mM NaCl, with (solid line) or without (dashed line) 3 mM imidazole. Compression rate, $1 \text{ \AA}^2/\text{min}$ per molecule; 25°C for all compressions.

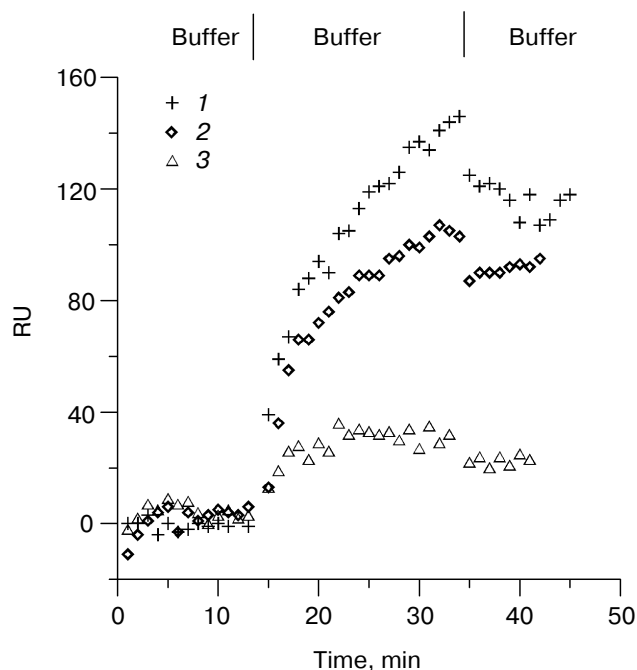


Fig. 3. Inhibitory effect of imidazole on the binding of P1 to NTA chip. The NTA-chip surface was first blocked with 1% BSA. After three cycles of buffer wash, the binding of P1 to NTA chip was carried out in the buffer (20 mM Tris-HCl, pH 7.4, 100 mM NaCl, 1 mM Ni^{2+} , 1 mM Ca^{2+} , 1 mM Mg^{2+}) without imidazole (1), with 30 mM imidazole (2), or with 100 mM imidazole (3).

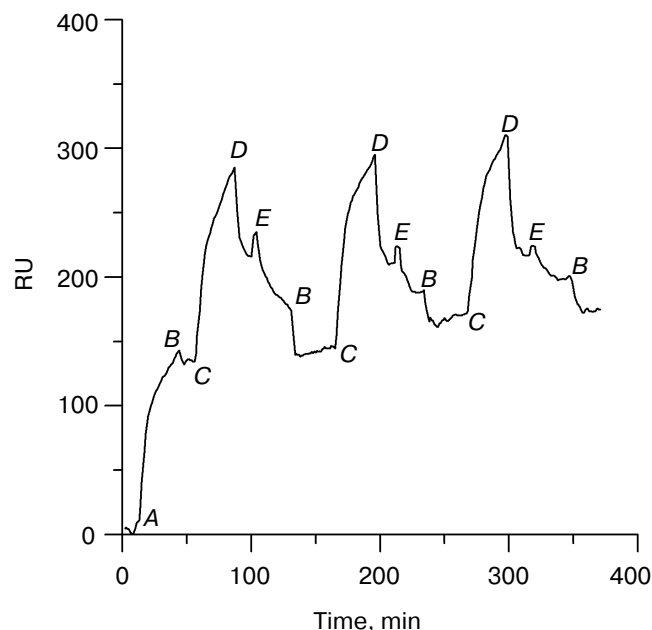


Fig. 4. Regeneration of an NTA-chip. After P1 was bound to the NTA-chip in 1 mM Ni^{2+} , the surface bound P1 was cleaned with 10 mM EDTA, and then the surface binding activity was regenerated by 30 min incubation with 1 mM Ni^{2+} at room temperature. This process was repeated for three times. *A* is adding 1% BSA for blocking; *B* is changing buffer to 1 mM Ni^{2+} ; *C* is adding P1; *D* is washing the chip with 1 mM Ni^{2+} ; *E* is washing with 10 mM EDTA.

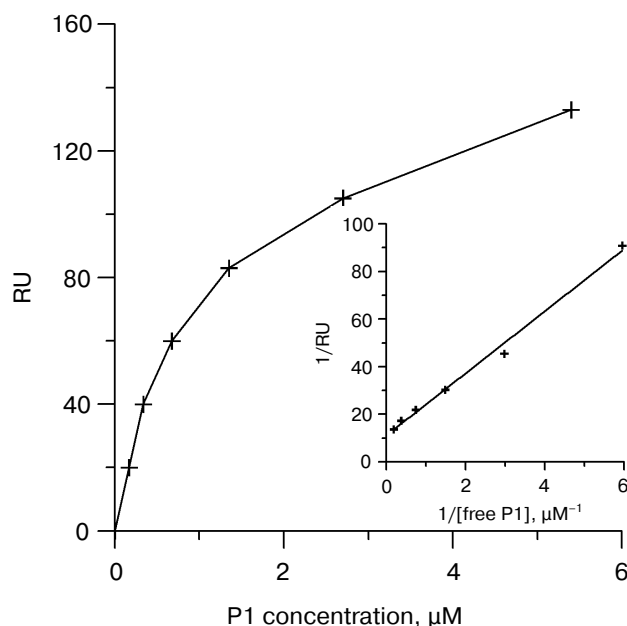


Fig. 5. Determination for the dissociation constant of P1. A series of concentrations of P1 were added to the sample chamber and the bound amount after buffer wash was recorded. The running buffer is 20 mM Tris-HCl, pH 7.4, 100 mM NaCl, 1 mM Ni^{2+} , 1 mM Ca^{2+} , 1 mM Mg^{2+} . The inset graph shows the plot used to calculate the apparent dissociation constant.

we can see that the NTA-chip can be reused, but with a partial loss of its activity of about 20%. After each wash of EDTA, the bound amount of P1 decreases to 80% of its maximum bound amount. Since EDTA is a specific chelator of Ni^{2+} and the specific binding of P1 to NTA only occurs in the presence of Ni^{2+} , the main reason of activity loss may be due to the unspecific adsorption of P1 to the chip.

Derivation of apparent dissociation constant of P1. P1 with concentrations from 0.17 to 5.4 μM was added into chamber separately to obtain the apparent dissociation constant of P1. The relationship between concentration of bound P1 (expressed by RU) and concentration (C) of free P1 in bulk is shown in Fig. 5. The inset plot of $1/R$ versus $1/C$ determines the semi-saturating concentration of P1. K_d was calculated to be 1.17 μM .

The specific binding of integrin to P1. As GRGDSP is a competitor of the binding between integrin with P1, so the inhibitory effect of GRGDSP on the binding of integrin to P1 was examined. Adding peptide GRGDSP into the sample chamber can cause a significant decrease in binding of integrin to P1, as shown in Fig. 6. From the curves we can see that about half of the bound integrin still remained on the surface after washing when the buffer did not contain GRGDSP. In contrast, almost all the bound integrin can be eluted away when washing with

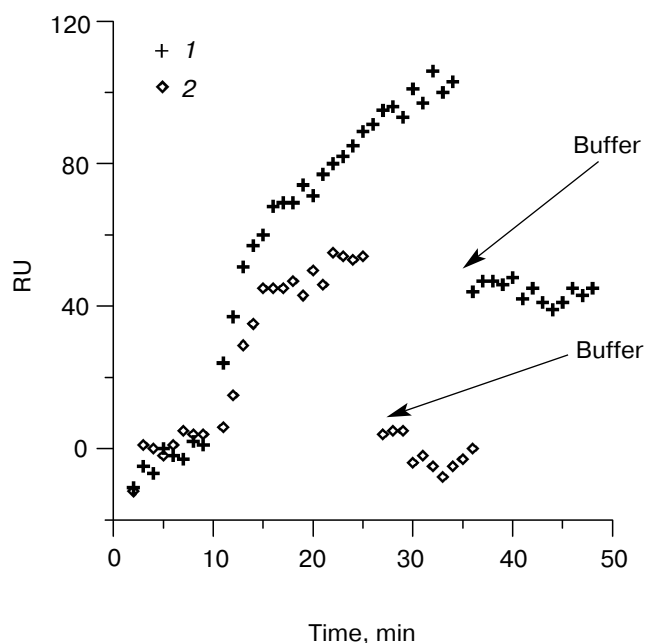


Fig. 6. Inhibitory effect of GRGDSP on integrin binding to P1. Integrin binds to P1 in the absence (1) or in the presence of 17 μM GRGDSP (2). Running buffer is 20 mM Tris-HCl, pH 7.4, 100 mM NaCl, 1 mM Ca^{2+} , 1 mM Mg^{2+} .

buffer containing 17 μM GRGDSP. The amounts that could be eluted out in the two buffers are almost equal, which are adsorbed onto P1. This suggests that binding of integrin to the sensor chip contains composite effects: specific interaction and unspecific adsorption. The binding in specific interaction is stable and cannot be eluted out by buffer, but adsorption is weak and can be eluted out.

Effect of divalent cations on integrin–ligand binding.

As divalent cations have distinct effects on integrin binding affinity [6–14], experiments were carried out to investigate the effect of various divalent cations on the binding activity of integrin to its RGD ligand. As shown in Fig. 7, in the presence of 1 mM EGTA the bound amount is only about 15 RU, indicating that EGTA can eliminate almost all integrin specific binding. Compared to the bound amount of 50 RU in the presence of 1 mM Ca^{2+} and 1 mM Mg^{2+} , the bound amount of dialyzed integrin was increased to 70 RU in buffer C (without Ca^{2+}). If 1 mM Mn^{2+} was present in buffer, the bound amount of integrin increased whether Ca^{2+} was present or not. In the both cases, the bound amount of integrin increased to 80 RU.

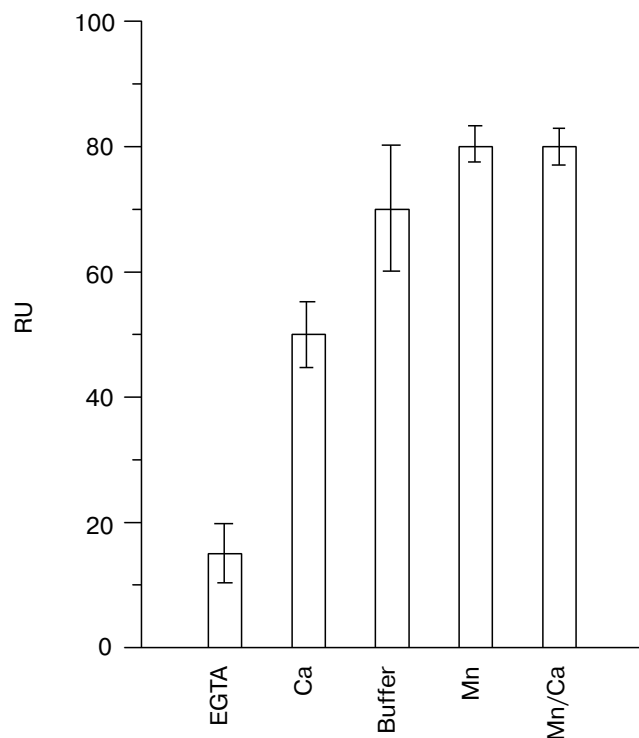


Fig. 7. Effects of divalent cations on integrin ligand binding activity. After P1 is immobilized on the NTA-chip, the binding of dialyzed integrin was carried out in the buffer 20 mM Tris-HCl, pH 7.4, 100 mM NaCl, 1 mM Mg^{2+} with EGTA or different cations as indicated in the figure.

DISCUSSION

The binding activity of NTA-lipids can be tested through imidazole binding. As shown in Fig. 2, the area per NTA-DOGS molecule has an increase of about 17 \AA^2 in the presence of 3 mM imidazole, and the isotherm with 3 mM imidazole has a nearly parallel shift compared with the one without imidazole. This suggests that imidazole binds to the NTA-lipid and such binding causes an increase in the headgroup size. Binding of imidazole to NTA-DOGS is specific and tight as imidazole still binds on NTA-DOGS even at a surface pressure of 45 mN/m.

The NTA-chip can immobilize His₆-tagged protein on the chip surface through the tight binding of NTA-DOGS with histidine. The dissociation constant of His-tagged protein to Ni-NTA has been measured to be 10^{-13} M at pH 8 [45], and it is stronger than most antibody bindings, which typically range from 10^{-6} to 10^{-9} M [46]. But binding of NTA-lipid to His-tagged protein is much weaker. A binding between His-tagged peptide containing six histidines and NTA-lipid vesicle has been reported to have a dissociation constant of 3 μM [47]. The binding of P1 is determined by the His-tag binding to NTA molecule, because most P1 remains to bind onto the sensor in the presence of 30 mM imidazole, and the surface binding ability of P1 can be abolished by 100 mM imidazole, as shown in Fig. 3. The apparent dissociation constant we got is in the range of μM , which is closed to that obtained from peptide interaction with NTA-lipid vesicles [47]. As P1 binds to NTA chip through its N-terminal, it indicates that under the support of carbon chain the RGD headgroup (C-terminal) will remain for further investigation.

Integrin has a ligand-binding pocket, which has a distance from the surface of 1.1–3.2 nm investigated by binding of integrin to RGDF with different length of spacer [48], or 0.75–0.85 nm detected by NMR [49]. To provide an effective binding of RGD to integrin, a peptide with six histidines and a spacer of ϵ -aminohexanoic-GG linked RGDS ligand was synthesized. The maximum length of the spacer is calculated to be 2.2 nm from known bond length and bond angle. This distance is sufficient to provide RGD peptide to enter the ligand binding pocket if the peptide is properly immobilized onto the chip. As described in the previous paragraph, the six histidines in the N-terminal of P1 can interact with NTA-chip specifically, so the orientation of P1 on the sensor chip can be ensured. From Fig. 6, it can be observed that in the presence of free RGD peptide, the specific binding of integrin is totally inhibited. This indicates RGD peptide has a competitive effect on the binding of P1 to integrin and suggests that P1 binds to the NTA-chip in a manner that the RGD headgroup of P1 is extended out. The extended RGD ligand can enter the binding pocket of integrin, and then promote a specific binding of RGD group to integrin. As there is flexibility in the carbon

chain, the real depth of integrin RGD binding site should be less than 2.2 nm.

Divalent cations are very important in regulating integrin $\alpha_{IIb}\beta_3$ ligand binding activity. As reported by previous studies [6-15], Ca^{2+} is essential for integrin ligand binding and the binding of Ca^{2+} to the second affinity site has different effect on integrin ligand binding. Our experiments showed that in the buffer with 1 mM EGTA or 1 mM Ca^{2+} or without Ca^{2+} , integrin has different bound amount. As shown in Fig. 7, integrin has little binding after adding 1 mM EGTA in the buffer, and the binding amount of integrin in buffer C increased by 40% to that in 1 mM Ca^{2+} . This suggests that Ca^{2+} is required for integrin binding and the increased binding ability of integrin is mainly caused by removal of Ca^{2+} binding to the low affinity sites.

Mn^{2+} can promote RGD ligands binding to the resting form of integrin [50]. As shown in Fig. 7, integrin binding amount was increased to 80 RU in 1 mM Mn^{2+} buffer, no matter whether Ca^{2+} was present or absent in the buffer. This indicates that adding 1 mM Mn^{2+} can eliminate the inhibitory effect on integrin ligand binding ability induced by Ca^{2+} binding to the low affinity sites. Though the binding sites of Mn^{2+} and Ca^{2+} are still not clear, the loss of Ca^{2+} inhibitory effect after adding Mn^{2+} suggests Mn^{2+} has a regulatory role in Ca^{2+} binding to the low affinity binding sites. This has some relative accordance with some previous findings that Mn^{2+} might bind to the low affinity cation binding site of integrin [51-53]. Our results give a further implication that Mn^{2+} may bind to the low affinity Ca^{2+} binding site, and the binding activity of this site to Mn^{2+} is larger than that to Ca^{2+} . The occupancy of low affinity Ca^{2+} binding sites by Mn^{2+} can restrain Ca^{2+} from binding to the low affinity binding site, thus eliminating the inhibitory effect of Ca^{2+} .

In conclusion, we developed an NTA-chip and synthesized a histidine-tagged peptide P1. P1 was immobilized on the NTA-chip with a proper orientation, and then was used to study the effect of divalent cations on integrin ligand binding ability. The result shows that Ca^{2+} binding to the low affinity binding sites decreases the binding ability of integrin to ligand, while the presence of Mn^{2+} can eliminate this inhibitory effect. The binding site of Mn^{2+} may be the low affinity Ca^{2+} binding site. It also suggests that divalent cations are an important factor in regulating integrin ligand binding affinity and will play an important role in regulating the physiological role of integrin.

This work was supported by the National Natural Sciences Foundation of China.

REFERENCES

- Benett, J. S., Vilaire, G., and Cines, D. B. (1982) *J. Biol. Chem.*, **257**, 8049-8054.
- Plow, E. F., and Ginsberg, M. H. (1981) *J. Biol. Chem.*, **256**, 9477-9482.
- Thiagarajan, P., and Kelly, K. L. (1988) *J. Biol. Chem.*, **263**, 3035-3038.
- Fujimoto, T., Ohara, S., and Hawiger, J. (1982) *J. Clin. Invest.*, **69**, 1212-1222.
- Ruoslahti, E., and Pierschbacher, M. D. (1986) *Cell*, **44**, 517-518.
- Suehiro, K., Smith, J. W., and Plow, E. F. (1996) *J. Biol. Chem.*, **271**, 10365-10371.
- Fitzgerald, L. A., and Philips, D. R. (1985) *J. Biol. Chem.*, **260**, 1366-1374.
- Rivas, G. A., and Gonzalez-Rodriguez, J. (1991) *Biochem. J.*, **276**, 35-40.
- Hu, D. D., Barbas III, C. F., and Smith, J. W. (1996) *J. Biol. Chem.*, **271**, 21745-21751.
- Dransfield, I., Cabanas, C., Craig, N., and Hogg, A. (1992) *J. Cell. Biol.*, **116**, 219-226.
- Edwards, J. G., Hameed, H., and Campbell, G. (1988) *J. Cell Sci.*, **89**, 507-513.
- Kirchhofer, D., Gailit, J., Ruoslahti, E., Grzesiak, J., and Pierschbacher, M. D. (1990) *J. Biol. Chem.*, **265**, 18525-18530.
- Kunicki, T. J., Annis, D. S., Deng, Y. J., Loftus, J. C., and Shattil, S. J. (1996) *J. Biol. Chem.*, **271**, 20315-20321.
- Smith, J. W., Piotrowicz, R. S., and Mathis, D. (1994) *J. Biol. Chem.*, **269**, 960-967.
- Michishita, M., Videm, V., and Arnaout, M. (1993) *Cell*, **72**, 857-867.
- Sui, S. F., Xiao, C. D., Zhou, Y., Xie, W. Z., and Liang, J. F. (1999) *Adv. Biosensors*, **4**, 123-137.
- Salamon, Z., Wang, Y., Tollin, G., and Macleod, H. A. (1994) *Biochim. Biophys. Acta*, **1195**, 267-275.
- Sui, S. F., Sun, Y. T., and Mi, L. Z. (1999) *Biophys. J.*, **76**, 333-341.
- Haussling, L., Ringsdorf, H., Schmitt, F. J., and Knoll, W. (1991) *Langmuir*, **7**, 1837-1840.
- Striebel, Ch., Brecht, A., and Gauglitz, G. (1994) *Biosensors Bioelectron.*, **9**, 139-146.
- Morgan, H., Taylor, D. M., and D'Silva, C. (1992) *Thin Solid Films*, **209**, 112-126.
- Toth, A., Kiss, E., Herberg, F. W., Gergely, P., Hartshorne, D. J., and Erdodi, F. (2000) *Eur. J. Biochem.*, **267**, 1687-1697.
- Mernagh, D. R., Janscak, P., Firman, K., and Kneale, G. G. (1998) *Biol. Chem.*, **379**, 497-503.
- Tsoi, P. Y., Yang, J., Sun, Y. T., Sui, S. F., and Yang, M. S. (2000) *Langmuir*, **16**, 6590-6596.
- Soulages, J. L., Salamon, Z., Wells, M. A., and Tollin, G. (1995) *Proc. Natl. Acad. Sci. USA*, **92**, 5650-5654.
- Salamon, Z., and Tollin, G. (1996) *Biophys. J.*, **71**, 858-867.
- Heyse, S., Ernst, O. P., Dienes, Z., Hofmann, K. P., and Vogel, H. (1998) *Biochemistry*, **37**, 507-522.
- Hochuli, E., Döbeli, H., and Schacher, A. (1987) *J. Chromatogr.*, **411**, 177-184.
- Schmitt, L., Dietrich, Ch., and Tampé, R. (1994) *J. Am. Chem. Soc.*, **116**, 8485-8491.
- Dietrich, Ch., Schmitt, L., and Tampé, R. (1995) *Proc. Natl. Acad. Sci. USA*, **92**, 9014-9018.
- Dietrich, Ch., Boscheinen, O., Scharf, K., Schmitt, L., and Tampé, R. (1996) *Biochemistry*, **35**, 1100-1105.
- Dorn, I. T., Pawlitschko, K., Pettinger, S. C., and Tampé, R. (1998) *Biol. Chem.*, **379**, 1151-1159.

33. Kubalek, E. W., LeGrice, S. F. J., and Brown, P. O. (1994) *J. Struct. Biol.*, **113**, 117-123.
34. Kubalek, E. W., Brown, R. E., Celia, H., and Milligan, R. A. (1998) *Proc. Natl. Acad. Sci. USA*, **95**, 8040-8045.
35. Celia, H., Kubalek, E. W., Milligan, R. A., and Teyton, L. (1999) *Proc. Natl. Acad. Sci. USA*, **96**, 5634-5639.
36. Lévy, D., Mosser, G., Lambert, O., Moeck, G. S., Bald, D., and Rigaud, J. (1999) *J. Struct. Biol.*, **127**, 44-52.
37. Sigal, G. B., Bamdad, C., Barberis, A., Strominger, J., and Whitesides, G. M. (1996) *Analyt. Chem.*, **66**, 490-497.
38. Nieba, L., Nieba-Axmann, S. E., Persson, A., Hämäläinen, M., Edebratt, F., Hansson, A., Lidholm, J., Magnusson, K., Karlsson, A. F., and Plückthun, A. (1997) *Analyt. Biochem.*, **252**, 217-228.
39. Fitzgerald, L. A., Leung, B., and Phillips, D. R. (1985) *Analyt. Biochem.*, **151**, 169-177.
40. Sackmann, E. (1996) *Science*, **271**, 43-48.
41. Xiao, C. D., and Sui, S. F. (1999) *Eur. Biophys. J.*, **28**, 151-157.
42. Haldane, J. B. S. (1957) *Nature*, **179**, 832.
43. Lu, Y. J., Xia, X. F., and Sui, S. F. (2001) *Biochim. Biophys. Acta*, **1521**, 308-316.
44. Hainfeld, J. F., Liu, W. Q., Halsey, M. R., Freimuth, P., and Powell, R. D. (1999) *J. Struct. Biol.*, **127**, 185-198.
45. Schmitt, J., Hess, H., and Stunnenberg, H. (1993) *Mol. Biol. Rep.*, **18**, 223-230.
46. Harlow, E., and Lane, D. (1988) *Antibodies: A Laboratory Manual*, Cold Spring Harbor Laboratory Press, Cold Spring Harbor, N.Y., pp. 27-28.
47. Dorn, I. T., Neumaier, K. R., and Tampé, R. (1998) *J. Am. Chem. Soc.*, **121**, 2753-2763.
48. Beer, J. H., Springer, K. T., and Collier, B. S. (1992) *Blood*, **79**, 117-128.
49. Pfaff, M., Rangemann, K., Müller, B., Gurrath, M., Müller, G., Kessler, H., Timpl, R., and Engel, J. (1994) *J. Biol. Chem.*, **269**, 20233-20238.
50. Yan, B., Hu, D. D., Knowles, S. K., and Smith, J. W. (2000) *J. Biol. Chem.*, **275**, 7249-7260.
51. Brass, L. F., and Shattil, S. J. (1982) *J. Biol. Chem.*, **257**, 14000-14005.
52. Phillips, D. R., and Baughan, A. K. (1983) *J. Biol. Chem.*, **258**, 10240-10246.
53. Steiner, B., Cousot, D., Trzeciak, A., Gillesen, D., and Hadvary, P. (1989) *J. Biol. Chem.*, **264**, 13102-13108.